Heliyon 10 (2024) e28364

Contents lists available at ScienceDirect

Heliyon

journal homepage: www.cell.com/heliyon

Research article

Plumbagin induces ferroptosis in colon cancer cells by regulating p53-related SLC7A11 expression

Bingyi Wang [a,1,**], Weiqi Kong [a,1,*], Lixin Lv [b], Zhiqiang Wang [a]

[a] Department of General Surgery, Tongren Hospital, Shanghai Jiao Tong University School of Medicine, Shanghai, China
[b] Department of Hematology, Tongji Hospital, Tongji University School of Medicine, Shanghai, China

ARTICLE INFO

Keywords:
Colon cancer
Plumbagin
Ferroptosis
p53/SLC7A11

ABSTRACT

Objective: This study examined the mechanism through which plumbagin induces ferroptosis of colon cancer cells.
Methods: CCK-8 assay was performed to examine the viability of colon cancer cells (SW480 and HCT116 cells) after they were treated with 0-, 5-, 10-, 15- and 20-μmol/L plumbagin. Colony formation assay and Transwell assay were used to examine the effects of 15-μmol/L plumbagin on the proliferation, invasive ability. The ferroptosis of SW480 and HCT116 cells and the expression of p-p53, p53 and SLC7A11 were analysed. The effects of blocking necrosis, apoptosis and ferroptosis on the anti-cancer effects of plumbagin were examined. After p53 was silenced, the effects of plumbagin on proliferation, invasion, ferroptosis and SLC7A11 expression were assessed. A tumour-bearing nude mouse model was used to examine the effects of p53 silencing and/or plumbagin on tumour growth, ferroptosis and SLC7A11 expression.
Results: Plumbagin inhibited the proliferation of SW480 and HCT116 cells and their invasive and colony-forming abilities. It increased Fe^{2+} levels but significantly decreased GSH and GPX4 levels. When ferroptosis was inhibited, the effects of plumbagin on colon cancer cells were significantly alleviated. Plumbagin promoted the expression and phosphorylation of p53 and inhibited the mRNA and protein levels of SLC7A11. Silencing of p53 counteracted the effects of plumbagin on the ferroptosis and biological behaviour of SW480 and HCT116 cells. In mouse models of colon cancer, silencing of p53 attenuated the tumour-suppressing effects of plumbagin as well as its inhibitory effects on the protein level of SLC7A11 and restored the expression of GSH and GPX4.
Conclusion: Plumbagin promotes ferroptosis and inhibits cell proliferation and invasion by decreasing the protein expression of SLC7A11 through p53.

1. Introduction

Every year, an estimated 1.1 million cases of colon cancer are diagnosed all over the world, making it the fifth most common cancer. Approximately 0.57 million patients die from colon cancer annually, accounting for 5.8% of all cancer-related deaths [1]. Although

* Corresponding author. Department of General Surgery, Tongren Hospital, Shanghai Jiao Tong University School of Medicine, No.1111, Xianxia Rd, Shanghai, China.
** Corresponding author. Department of General Surgery, Tongren Hospital, Shanghai Jiao Tong University School of Medicine, No.1111, Xianxia Rd, Shanghai, China.
E-mail addresses: WBY4230@shtrhospital.com (B. Wang), KWQ4499@shtrhospital.com (W. Kong).
[1] Bingyi Wang and Weiqi Kong are co-corresponding authors.

https://doi.org/10.1016/j.heliyon.2024.e28364
Received 22 August 2023; Received in revised form 18 March 2024; Accepted 18 March 2024
Available online 21 March 2024

surgery and chemotherapy are common treatments for colon cancer, novel immunotherapies are now being more frequently utilized in clinical practice. Despite this advancement, the prognosis for colon cancer is still bleak [2,3]. Many patients miss out on the best chance for surgery when they are first diagnosed, potentially leading to the spread of cancer [4,5]. Consequently, developing new drugs that can effectively treat colon cancer is important.

Compounds of natural origin have evident tumour-suppressing effects and a low resistance potential [6,7]. Plumbagin ($C_{11}H_8O_3$) is a quinone derived from the whole plant of *Plumbago indica* L. or the root of *P. zeylanica* Linn. Recent studies have shown that plumbagin has excellent therapeutic effects against breast cancer and other cancer [8–10]. Although plumbagin can block colon cancer cell cycle in vitro [11], its effects on cell migration and invasion and its mechanism of action remain unclear.

Abnormal ferrous iron can catalyse the peroxidation of unsaturated fatty acids on the cell membrane, inducing ferroptosis [12]. GPX4 is a selenoprotein that efficiently catalyses the reduction of peroxidised phospholipids. Glutathione (GSH) depletion-induced inactivation of GPX4 specifically triggers ferroptosis. When ferroptosis is triggered, it inhibits tumour cell proliferation, drug resistance and invasion [13,14]. SLC7A11 is involved in the synthesis of GSH through cystine and inhibits ferroptosis. A bioinformatic study demonstrated that SLC7A11 was overexpressed in colon cancer and its regulatory effects on ferroptosis were related to metastasis-associated chemokines [15]. In addition, plumbagin and deletion of SLC7A11 have been shown to enhance ferroptosis in lung and breast cancers [16,17]. However, whether plumbagin can induce ferroptosis in colon cancer remains unclear.

The present study aimed to examine the impact of plumbagin on colon cancer cells and elucidate its underlying mechanism. The findings of this study may provide novel insights into the management of colon cancer.

2. Materials and methods

2.1. Cells culture

The normal colonic epithelial cell line NCM460 (CL-0393) and the colon cancer cell lines SW480 (wild-type p53, CCL-228) and HCT116 (wild-type p53, CCL-247 EMT) were purchased from ATCC (USA). The cells were all cultured in DMEM (Gibco, USA) supplemented with 10% fetal bovine serum (FBS) and 100 × penicillin-streptomycin solution in an incubator at 37 °C with 5% CO_2 and 95% humidity.

The cells were treated with plumbagin (99%, CFN90444; Wuhan ChemFaces Biochemical Co., Ltd., Wuhan, China) at final concentrations of 0, 5, 10, 15 and 20 μmol/L for 24, 48 and 72 h. Thereafter, plumbagin was used at a concentration of 15 μmol/L for subsequent experiments (72 h). To assess the safety of plumbagin, normal colonic epithelial cells (NCM460) were treated with 15-μmol/L plumbagin for 72 h. The resulting cell viability was 72.6 ± 7.1%, indicating that the dosage was relatively safe.

Before plumbagin treatment, the cells underwent treatment with the ferroptosis inhibitors Fer-1 (1 μmol/L, HY-100579, MedChemExpress) and Lip-1 (0.2 μmol/L, HY-132216) for 24 h. Additionally, the cells were pre-treated with 10 μmol/L Nec-1 (HY-15760) and 10 μmol/L Z-VAD-FMK (HY–16658B) for 24 h to inhibit necroptosis and pan-caspase apoptosis, respectively.

2.2. Cell transfection

For transfection, cells were assigned into the following groups: si-NC, si-NC + plumbagin, si-p53 and si-p53 + plumbagin. To examine the mechanism of action of plumbagin, p53 was silenced before plumbagin treatment (15 μmol/L). si-p53 and corresponding si-NC were synthesized by GenePharma Co., Ltd. (China). To prepare a transfection complex, the procedure involved combining 25 μL of reagent A with 25 μL of reagent B and mixing them thoroughly by aspirating the mixture 10 times using a pipette, followed by a 15-min incubation period. After that, cells were transfected with 50 μL of the resulting transfection complex.

2.3. CCK-8 assay

Transfected cells (100 μL; 5×10^4 cells/mL) were placed in 96-well plates. Following incubation, CCK-8 solution was added to cells and the plates were gently mixed at 37 °C for 1 min to ensure uniform distribution. After 2 h of incubation (for dehydrogenation reaction), optical density (OD) was measured at 450 nm using the Feyond-A500 microplate reader (AS-19070-00, Aosheng, AS-19070-00, China).

2.4. Colony formation assay

After digestion and resuspension, 200 single cells were evenly seeded in the medium of each well and cultured for 14 days. The medium was replaced every 2–3 days. After the appearance of macroscopic colonies, the cells were rinsed with PBS twice. Following that, the cells were treated with 4% PFA for 15 min and stained with Giemsa for 20 min. After gently washing away any excess stain, the cells were left to dry. Once dry, a transparent film with grids was placed over the inverted plate. The number of colonies with >20 cells was recorded, and the relative clone formation efficiency was normalised to that of the si-NC group.

2.5. Transwell assay

Matrigel (diluted at a ratio of 1:8; Corning, USA) and complete DMEM (20% FBS) was added to the lower Transwell chamber. They were then incubated at 37 °C for 30 min. Cells were starved in serum-free DMEM (5×10^4 cells/mL) at 37 °C for 24 h. Following

digestion, 100 μL of the cell suspension (5×10^4 cells/mL) was added to the upper Transwell chamber. 24 h later, non-invasive cells were removed, whereas invasive cells were fixed and stained with 0.1% crystal violet. Thereafter, the number of invaded cells was recorded in five random fields.

2.6. Detection of unstable Fe2+ ions

FerroOrange probe (MX4559, MKbio, China) was used to detect unstable Fe^{2+} ions. Frozen FerroOrange was incubated at 25 °C for 30 min and centrifuged at a low speed (using a microcentrifuge). The precipitated FerroOrange (24 μg) powder was dissolved in 35 μL of DMSO by mixing the solution 5 times. Next, the cell culture medium was used to obtain 1-mM FerroOrange stock solution. Cells were seeded in fluorescent petri dishes and incubated with the stock solution overnight at 37 °C with 5% CO_2. For laser microscopy, the excitation wavelength was set to 532 nm, while the emission wavelength was set to 572 nm, and the relative concentration of Fe^{2+} ions was calculated using siNC as Control.

3. ELISA

A 96-well plate was divided into the following compartments: blank wells (A, blank control; no sample or enzyme-labelling reagent was added; other steps were the same), standard wells (B; 50-μL standard solution was added) and sample wells (C; 10-μL sample and 40-μL diluent were added). An enzyme-labelling reagent (50 μL, 37 °C, 30 min) and chromogenic reagents A and B (50 μL each, 37 °C, 15 min, GSH assay kit, S0052, Beyotime, China) were successively added to all the wells under dark conditions. OD was measured at 450 nm, and the relative concentration of GSH in C wells was calculated and normalised to that in A and B wells. A GPX4 ELISA kit (EK-H12496, EK-Bioscience, China) was used to detect GPX4, and the procedure was similar to that used for detecting GSH.

3.1. qRT-PCR

Cells or tissues were treated with 400 μL of Trizol (Thermo Fisher, USA) in a 1.5-mL sterile RNase-free EP tube. After the samples were homogenised, 600 μL of Trizol was added and the samples were mixed for 5 min, followed by centrifugation of the cell or tissue lysates for 5 min at 12,000×*g* and 4 °C. A mixture of Trizol and chloroform in a 1:2 ratio was added to the RNA pellet, mixed for 15 s. The cDNA was then synthesized using the PrimeScript RT Reagent Kit (RR047A, Takara) at 37 °C for 15 min and 98 °C for 5 min. Subsequently, qPCR was carried out using SYBR Green (Takara, Japan) at 94 °C for 3 min, then 40 cycles of 94 °C for 15 s, 58 °C for 20 s, and 72 °C for 30 s. The mRNA levels of target genes was determined and normalised to that of β-actin using the $2^{-\Delta\Delta Ct}$ method. The primer sequences used for PCR are as follows: p53-F, 5′-TCCACACCCCCGCCC-3′; p53-R, 5′-CCTCACAACCTCCGTCATGT-3′; SLC7A11-F, 5′- TGAGAGCACGATGCATACACA-3′; SLC7A11-R, 5′-CCCTGCAGGTAACCTCCTTT-3′; GPX4-F, 5′- GGGACCATGTGCGCGTC-3′, GPX4-R, 5′-CTTCATCCACTTCCACAGCG-3′; β-actin-F, 5′-TTGCCCTGAGGCTCTTTTCC-3′; β-actin-R, 5′-AATGCCAGGGTACATGGTGG-3′.

3.2. Western blot

Samples were gathered and broken down in RIPA buffer (on ice, 30 min), and total proteins were extracted from the cell or tissue lysates via centrifugation (4 °C, 12000×*g*, 20 min). The proteins extracted were separated using a 10% sodium dodecyl sulfate-polyacrylamide gel and then transferred to a PVDF membrane, a semi-crystalline and non-reactive thermoplastic polymer with excellent piezoelectric properties [18]. The membrane was incubated with rabbit monoclonal primary antibodies against p-p53 (1:1000) (ab33889, Abcam, USA), p53 (1:1000) (ab32389, Abcam, USA), SLC7A11 (ab175186) and GPX4 (ab125066) at 4 °C overnight. The next day, the membrane was exposed to a secondary antibody (1:2000, ab6721) and incubated at 37 °C for 2 h and washed thrice with TBST. Blots were detected with an ECL kit from Solarbio, and the IPP6.0 software (Media Cybernetics, USA) was used to analyse the protein expression.

3.3. Xenotransplantation

Nude BALB/C mice (4 weeks old; Charles River. Co., LTD., China) were kept under 24 ± 1 °C and of 60 ± 5% humidity. They were randomly grouped with 4 mice in each group. 5×10^6 SW480 and HCT116 cells, transfected with either si-NC or si-p53, were suspended in 200 μL of PBS and then injected into the axillary regions of the nude mice. Tumour formation was observed after 5–7 days. On days 1 and 4 of weeks 2–4, the mice were injected with 2-mg/kg plumbagin intraperitoneally. After 4 weeks, the mice were euthanised and tumours were collected and weighed.

3.4. Statistical analysis

The experiments were conducted three times independently, and the results were presented as the mean ± SD. Statistical analysis was carried out using one-way ANOVA and the Tukey multiple comparison test in GraphPad Prism version 7.0. The *t*-test was used for comparing two groups, and the log-rank test was used to analyse survival. A P-value of <0.05 was considered significant.

4. Results

4.1. Plumbagin inhibited colon cancer cell growth and invasion

To examine the anti-cancer effects of plumbagin, colon cancer cells were treated with 0-, 5-, 10-, 15- or 20-μmol/L plumbagin. The results showed that treatment with plumbagin at concentrations of 5, 10, 15 and 20 μmol/L significantly inhibited the proliferation of colon cancer cells. Although these effects followed a dose-dependent trend in cells treated with ≤15-μmol/L plumbagin, they were found to be similar in cells treated with 15-μmol/L and 20-μmol/L plumbagin (Fig. 1A and 1B). In addition, the effects of plumbagin at 10, 15 and 20 μmol/L became more significant with increasing time (Fig. 1A and 1B). Therefore, colon cancer cells treated with 15-μmol/L plumbagin for 72 h were used for subsequent experiments. Treatment with 15-μmol/L plumbagin significantly attenuated the colony-forming (Fig. 1C and 1D) and invasive (Fig. 1E–1H) abilities of colon cancer cells. These results preliminarily validated the anti-cancer effects of plumbagin.

4.2. Plumbagin induced ferroptosis in colon cancer cells

Ferroptosis is characterised by an increase in intracellular unstable Fe2+ levels and a decrease in GSH and GPX levels. 15-μmol/L plumbagin increased Fe^{2+} levels by 3.5–4 folds (Fig. 2A and 2B) but significantly decreased GSH and GPX levels (Fig. 2C–2F) in colon cancer cells, suggesting plumbagin induced ferroptosis.

4.3. Inhibition of ferroptosis blocked the anti-cancer effects of plumbagin

To verify the key role of ferroptosis in the anti-cancer effects of plumbagin, colon cancer cells were pre-treated with Fer-1 and Lip-1 to inhibit ferroptosis (before plumbagin treatment). In addition, the cells were pre-treated with Nec-1 and Z-VAD-FMK to inhibit necroptosis and pan-caspase apoptosis, respectively. The results showed that Nec-1 did not have significant effects on the anti-proliferative effects of plumbagin, whereas Z-VAD-FMK attenuated the antiproliferative effects of plumbagin to some extent. On the contrary, both Fer-1 and Lip-1 significantly blocked the antiproliferative effects of plumbagin (Fig. 2G and 2H). Similarly, Nec-1 and Z-VAD-FMK had minimal effects on the colony-forming ability of colon cancer cells in the presence of plumbagin, whereas Fer-1 and Lip-1 significantly reversed the effects of plumbagin on colony formation (Fig. 2I and 2J). In addition, Z-VAD-FMK and Nec-1 had minimal effects on the invasive ability of colon cancer cells in the presence of plumbagin, whereas Fer-1 and Lip-1 significantly reversed the effects of plumbagin on cell invasion (Fig. 3A and 3B), indicating that inhibition of ferroptosis counteracted the effects of plumbagin on colon cancer cell, indicating that plumbagin exerts anti-cancer effects by inducing ferroptosis.

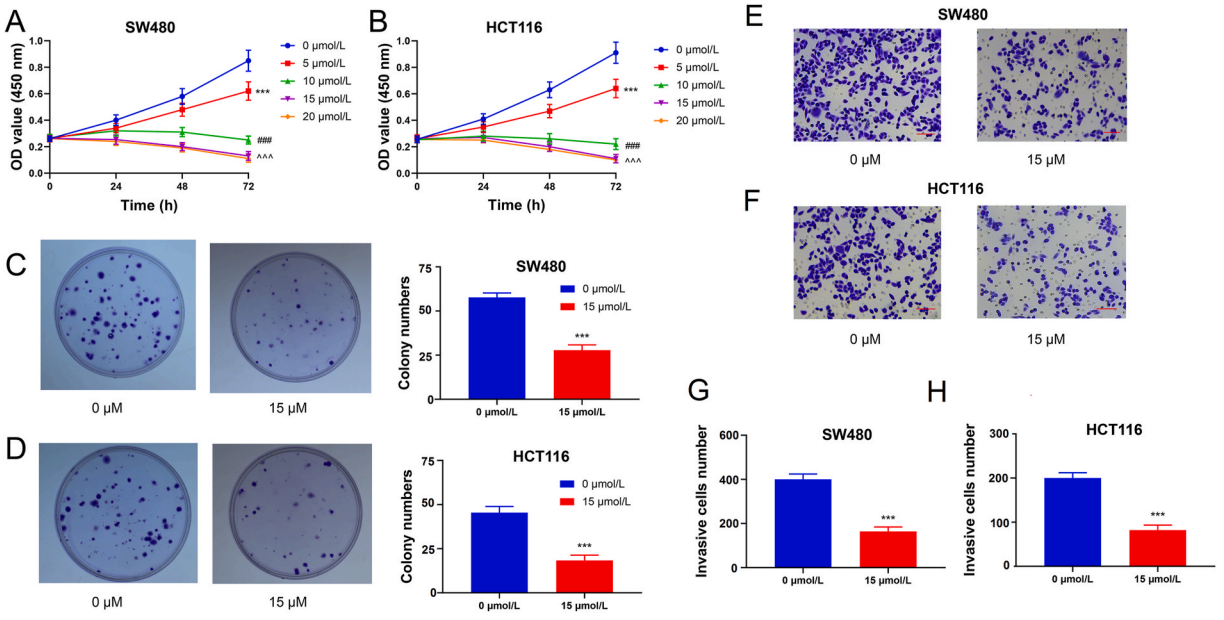

Fig. 1. Plumbagin inhibits colon cancer cell proliferation and invasion. (A–B) Effects of 0 μmol/L, 5 μmol/L, 10 μmol/L, 15 μmol/L, 20 μmol/L Plumbagin on the viability. (C–D) Effects of Plumbagin on the colony formation. (E–H) Effects of Plumbagin on invasion. Scar bar = 50 μm ***P < 0.001 vs. 0 μmol/L; ###P < 0.001 vs. 5 μmol/L; ^^^P < 0.001 vs. 15 μmol/L.

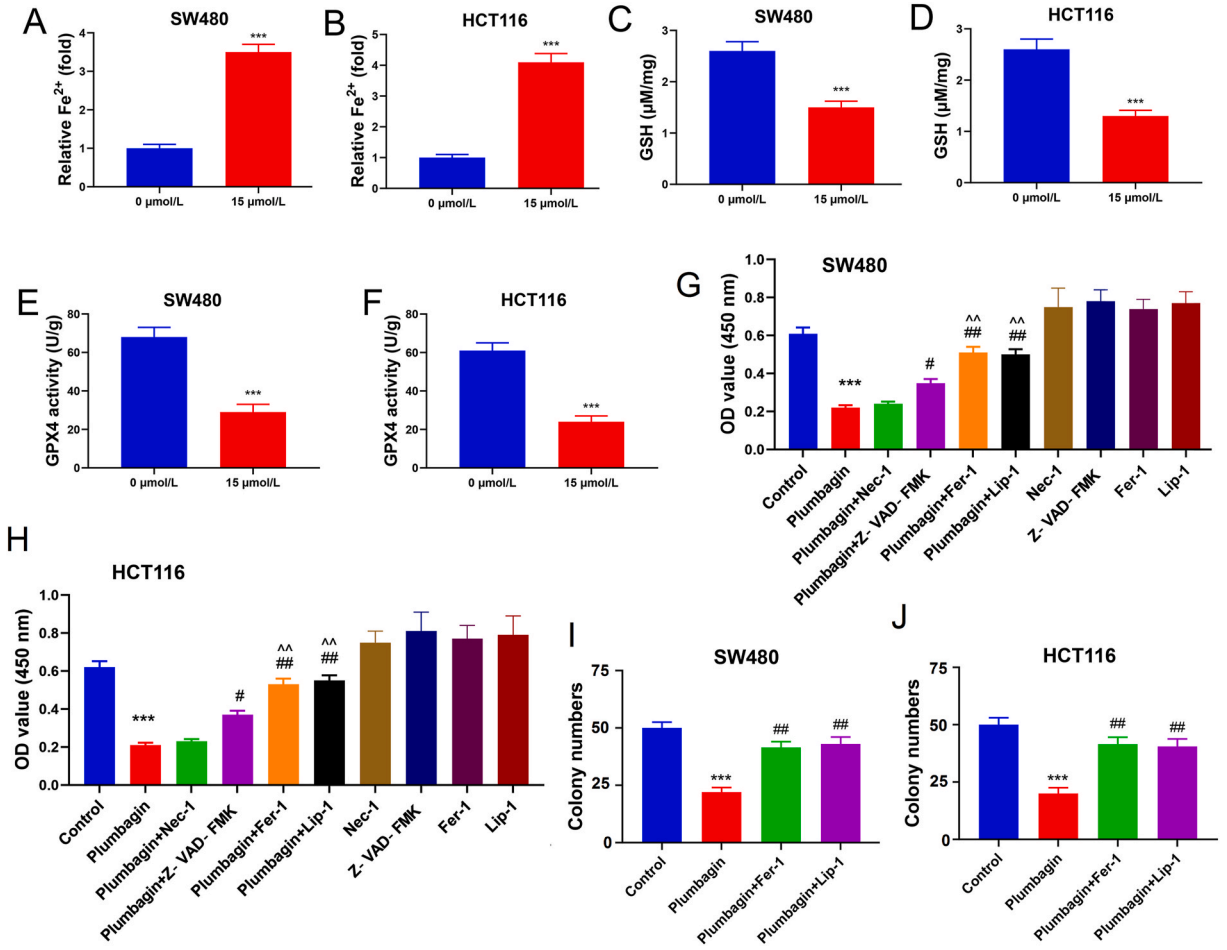

Fig. 2. Plumbagin induces ferroptosis in colon cancer cells and Inhibition of ferroptosis blocks the inhibitory effect of Plumbagin on colon cancer cell proliferation. (A–B) Effects of Plumbagin on Fe^{2+} concentration. (C–F) Effects of μmol/L Plumbagin on GSH and GPX4. (G–H) Effects of necroptosis inhibitor (Nec-1), pan-caspase apoptosis inhibitor (Z-VAD-FMK) and ferroptosis inhibitor (Fer-1 and Lip-1) on cell viability. (I–J) Effects of blocked necroptosis, pan-caspase apoptosis and ferroptosis on colony formation ability. ***P < 0.001 vs. 15 μmol/L or vs. control; #, ##P < 0.05, 0.01 vs. Plumbagin; ^^P < 0.01 vs. Z-VAD-FMK.

4.4. Plumbagin regulated the expression of the ferroptosis-related proteins p53 and SLC7A11

Treatment with plumbagin led to a 7-fold increase in the mRNA expression of p53 and a 4-fold increase in the protein expression of p-p53 and p53 (Fig. 3C and 3D). In addition, treatment with plumbagin significantly decreased the mRNA and protein expression of SLC7A11(Fig. 3E and 3F). These results suggest that plumbagin regulates the ferroptosis-related p53–SLC7A11 pathway.

4.5. Silencing of p53 blocked the anti-cancer effects of plumbagin

p53 induces ferroptosis by inhibiting the expression of SLC7A11. To verify that plumbagin induces ferroptosis through the p53–SLC7A11 pathway, p53 was silenced in colon cancer cells using siRNAs (Fig. 4A–4C). The proliferative ability of colon cancer cells was significantly increased in the si-p53 group and decreased in the si-NC + plumbagin group compared to the si-NC group. The proliferative ability of colon cancer cells in the si-p53 + plumbagin group was significantly higher than that in the si-NC + plumbagin group and significantly lower than that in the si-p53 group (Fig. 4D). Treatment with plumbagin inhibited the colony-forming ability of colon cancer cells. Silencing of p53 not only promoted colony formation but also reversed the effects of plumbagin (Fig. 4E). In addition, treatment with plumbagin inhibited the invasive ability of colon cancer cells, whereas silencing of p53 promoted cell invasion and reversed the effects of plumbagin on cell invasion (Fig. 5A and 5B). These results indicated that silencing of p53 counteracted the anti-cancer effects of plumbagin, suggesting that the anti-cancer effects of plumbagin are closely related to p53.

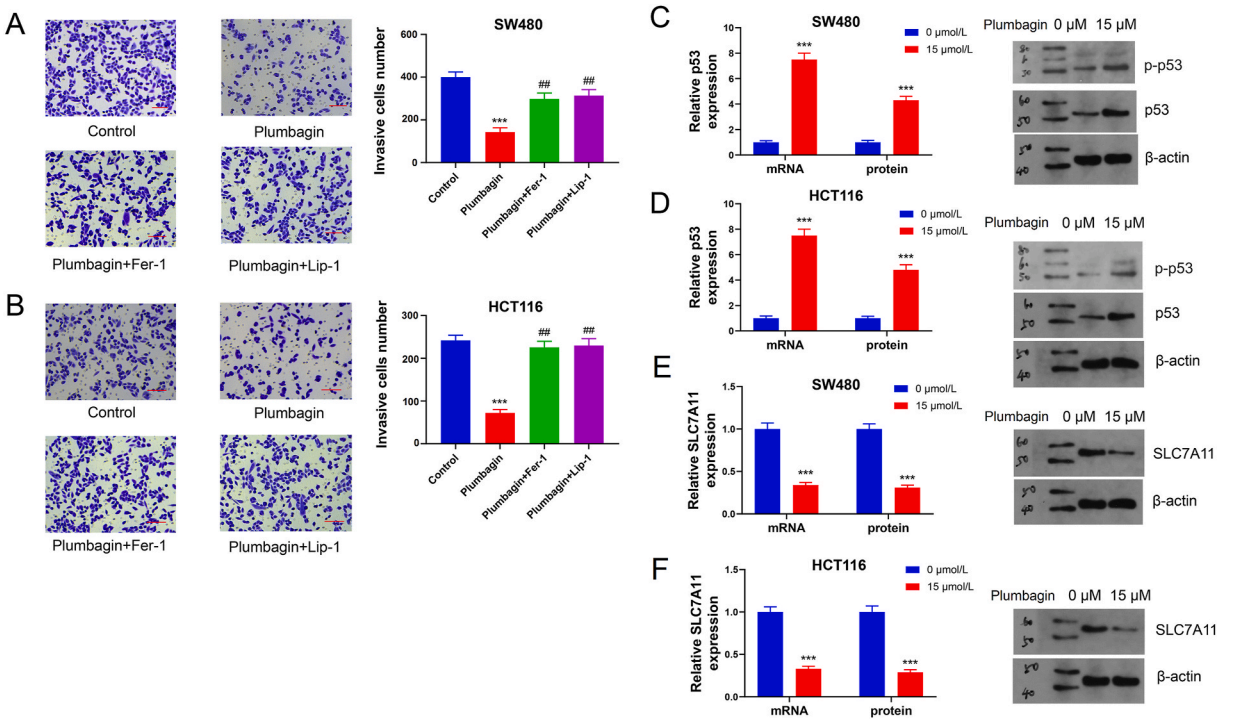

Fig. 3. Inhibition of ferroptosis blocks the inhibitory effect of Plumbagin on colon cancer cell invasion and Plumbagin regulates the expression of ferroptosis-related p53-SLC7A11 pathway. (A–B) Effects of necroptosis inhibitor (Nec-1), pan-caspase apoptosis inhibitor (Z-VAD-FMK) and ferroptosis inhibitor (Fer-1 and Lip-1) on invasion. (C–F) Effects of 15 μmol/L Plumbagin on p-p53 and p53 and SLC7A11 protein expression in cells. Scar bar = 50 μm ***P < 0.001 vs. control or vs. 15 μmol/L; #, ##P < 0.05, 0.01 vs. Plumbagin.

4.6. Silencing of p53 blocked plumbagin-induced ferroptosis and suppression of SLC7A11 expression

The effects of p53 silencing and/or plumbagin treatment on ferroptosis were examined in colon cancer cells. The mRNA and protein expression levels of SLC7A11 were lower in the si-NC + plumbagin group and higher in the si-p53 group than in the si-NC group. In addition, the mRNA and protein expression levels of SLC7A11 in the si-p53 + plumbagin group were increased compared to the si-NC + plumbagin group and decreased compared to the si-p53 group (Fig. 6A–6C). Plumbagin increased intracellular Fe2+ levels, whereas silencing of p53 significantly reversed the plumbagin-induced increase in Fe2+ levels (Fig. 6D). In addition, silencing of p53 reversed the plumbagin-induced decrease in GSH and GPX4 levels (Fig. 6E and 6F). These results indicated that silencing of p53 increased SLC7A11 expression and inhibited ferroptosis in the presence of plumbagin, suggesting that plumbagin induces ferroptosis by promoting the expression of p53.

4.7. Silencing of p53 blocked the anti-cancer effects of plumbagin and inhibition of SLC7A11 in vivo

To verify the anti-cancer effects of plumbagin and its p53-dependent regulatory effects on SLC7A11 expression *in vivo*, tumour-bearing nude mouse models were established using colon cancer cells transfected with si-NC or si-p53. Subsequently, mice with colon tumours were intraperitoneally injected with plumbagin. The results showed that treatment with plumbagin inhibited tumour growth *in vivo*, whereas silencing p53 not only promoted tumour growth but also significantly reversed the anti-tumour effects of plumbagin (Fig. 7A and 7B). Treatment with plumbagin inhibited the mRNA and protein expression of SLC7A11 in mouse tumour tissues, whereas silencing of p53 not only promoted SLC7A11 expression but also reversed the effects of plumbagin on SLC7A11 expression (Fig. 7C and 7D). These results indicated that the effects of plumbagin on colon tumour growth and SLC7A11 expression were closely related to p53 *in vivo*.

4.8. Silencing of p53 blocked the ferroptosis-inducing effect of plumbagin in vivo

Treatment with plumbagin decreased the levels of GSH and GPX4 in mouse tumour tissues, whereas silencing of p53 reversed these effects (Fig. 8A–8C). These results indicated that silencing of p53 blocked the ferroptosis-inducing effect of plumbagin *in vivo*. Fig. 8D shows a schematic diagram summarising the protocol of this study.

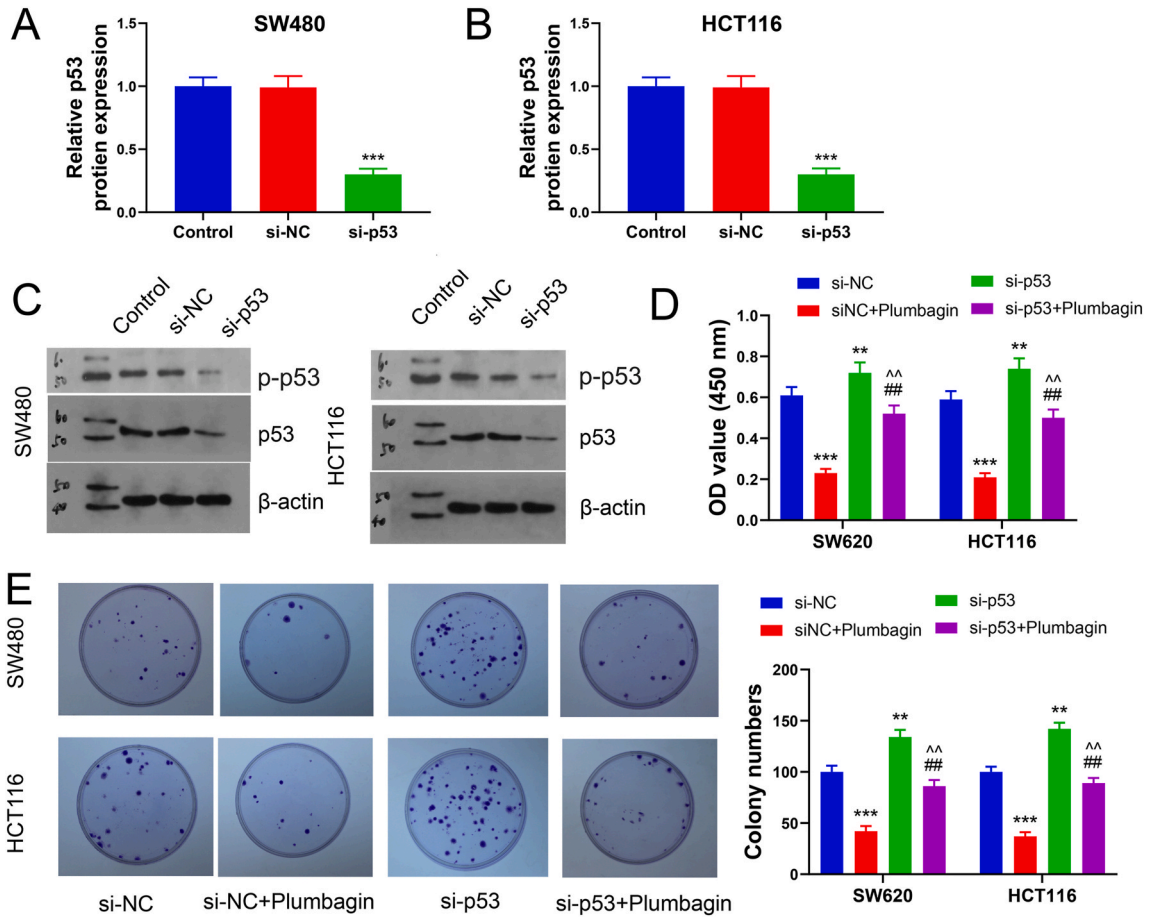

Fig. 4. Silencing p53 blocks the colon cancer inhibitory effect of Plumbagin. (A–C) Construction of a cellular model of p53 silencing. (D) Effects of silencing p53 and/or Plumbagin on cell viability. (E) Effects of silencing p53 and/or Plumbagin on colony formation ability. **, ***P < 0.01, 0.001 vs. si-NC; ##P < 0.01 vs. si-NC + Plumbagin; ^^P < 0.01 vs. si-p53.

5. Discussion

The pathogenesis of colon cancer is complex, involving environmental factors, genetic factors, inflammatory bowel disease and an interaction among these factors [19,20]. Surgery or combination chemotherapy is the primary treatment method for reducing the tumour burden and prolonging the survival of patients [21,22]. Approximately 60% of patients with colon cancer survive for five years or more [23,24]. However, colon cancer is difficult to detect at an early stage, and only 8–30% of patients with advanced colon cancer survived [25,26]. Therefore, understanding the mechanisms underlying colon cancer progression is important.

Many natural drugs are used as first-line treatment agents for several cancers. The use of these drugs is limited owing to their poor water solubility and potential for causing systemic reactions. These advantages can be addressed by modifying the route of administration [27,28]; therefore, natural drugs hold great promise in the treatment of cancer. As a natural quinone, plumbagin exhibits various biological activities, such as antibacterial [29], immunomodulatory [30] and pro-oxidative stress [31] activities. The anti-cancer effects of plumbagin have been shown in pancreatic cancer [32], liver cancer [33], oesophageal cancer [34], gastric cancer [35] and other digestive system tumours. Plumbagin also promoted apoptosis in colon cancer cells [36]. We also tested the effect of plumbagin on apoptosis in colon cancer cells (Supplementary Fig. 1) and the findings aligned with earlier research. However, the increase of apoptosis rate can't solely explain the decrease of cell viability. Therefore, it seems that the apoptosis was not the only mechanism of plumbagin and we explored the involvement of ferroptosis. In this study, plumbagin was found to inhibit the proliferative, colony-forming and invasive abilities of colon cancer cells, suggesting that Plumbagin showed significant efficacy in inhibiting the growth and spread of colon cancer.

Unlike normal cells, tumour cells rely on the trace element iron for their growth [37]. Excessive iron intake may increase the risk of breast cancer [38]. Some iron-chelating agents and drugs that increase iron-mediated cytotoxicity (e.g. sulfasalazine, statins and ferroptosis-causing artemisinin) have been shown to exert anti-tumour effects [39,40]. However, ferroptosis has dual effects on cancer. On the one hand, moderate ferroptosis is beneficial to the proliferation and metastasis of tumour cells [41]. On the other hand, depletion of GSH and inhibition of GPX4 significantly induce ferroptosis in tumour cells [42]. In addition, abnormally elevated levels

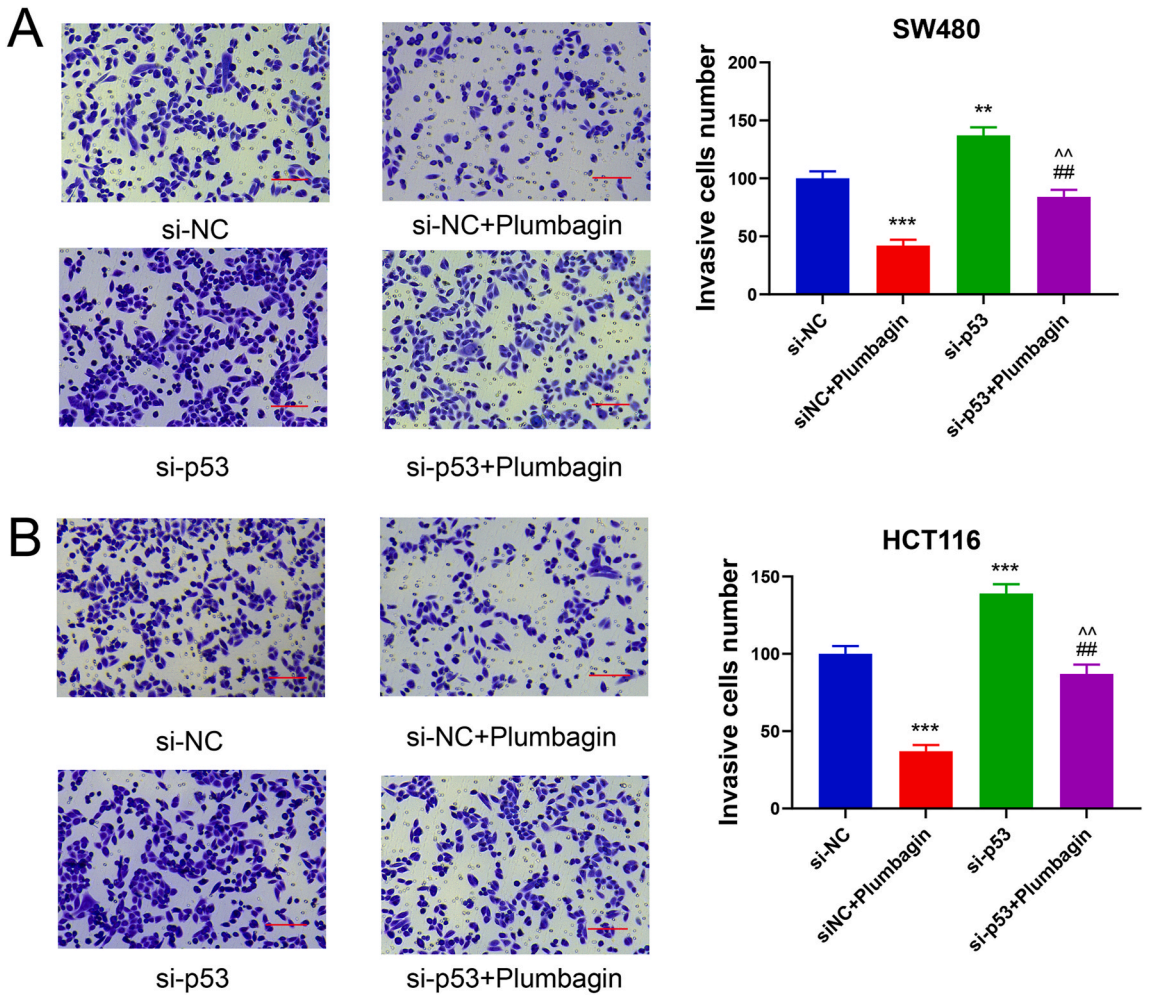

Fig. 5. Silencing of p53 blocks the inhibitory effect of Plumbagin on colon cancer cell invasion. (A–B) Effects of silencing p53 and/or Plumbagin on cell invasion. Scar bar = 50 μm **, ***P < 0.01, 0.001 vs. si-NC; ##P < 0.01 vs. si-NC + Plumbagin; ^^P < 0.01 vs. si-p53.

of ferroptosis can limit or inhibit the proliferative and metastatic abilities of tumour cells [43,44]. Therefore, targeting ferroptosis represents a novel therapeutic strategy for tumours. Plumbagin has been reported to enhance ferroptosis. For example, it can induce ferroptosis by inhibiting GPX4 and suppress tumour growth in nude mouse models of glioma [45]. The primary biochemical event that initiates ferroptosis is lipid peroxidation, while the enzyme-triggered rise in free radical generation, fatty acid availability, and lipid peroxidation also significantly contribute to inducing ferroptosis. The ferroptosis-inducing mechanism of plumbagin may be associated with its inherent pro-oxidative effects. First, inhibition of oxidative phosphorylation by plumbagin has the ability to enhance the production of ROS, which play a crucial role in inducing ferroptosis [46]. Second, inhibition of OXPHOS and the subsequent production of ROS can directly promote lipid peroxidation. ROS can damage the cell membrane via lipid peroxidation [47,48]. The damaged membrane disrupts cell integrity, eventually triggering ferroptosis. Third, dysfunction of OXPHOS affects iron metabolism, which is closely associated with ferroptosis [48,49]. Inhibition of OXPHOS causes the accumulation of free iron, which can participate in Fenton reactions and drive ferroptosis [48]. In this study, the levels of Fe^{2+}, GSH and GPX4 were evaluated to examine whether plumbagin regulated ferroptosis. Plumbagin increased Fe^{2+} levels but decreased GSH and GPX4 levels in SW480 and HCT116 cells. To verify the role of ferroptosis in the anti-cancer effects of plumbagin, colon cancer cells were treated with the ferroptosis inhibitors Fer-1 and Lip-1 before plumbagin treatment. In addition, the cells were pre-treated with Nec-1 and Z-VAD-FMK to inhibit necroptosis and pan-caspase apoptosis, respectively. Inhibition of ferroptosis significantly attenuated the effects of plumbagin on the proliferative and invasive abilities of colon cancer cells, indicating that plumbagin prevents the proliferation and spread of colon cancer cells, at least in part, by inducing ferroptosis.

SLC7A11 promotes the transfer of cysteine, a substrate for the synthesis of GSH, thereby alleviating ferroptosis-induced damage [50]. In a study, analysis of cancer data from TCGA, GEO and GEPIA databases showed that upregulated SLC7A11 was involved in the metastasis of colon cancer [15]. In addition, increased dietary intake of heme iron and SLC7A11 [51] and increased stability of SLC7A11 can promote the progression of colon cancer [52]. The transcription and expression of SLC7A11 are regulated by p53. An

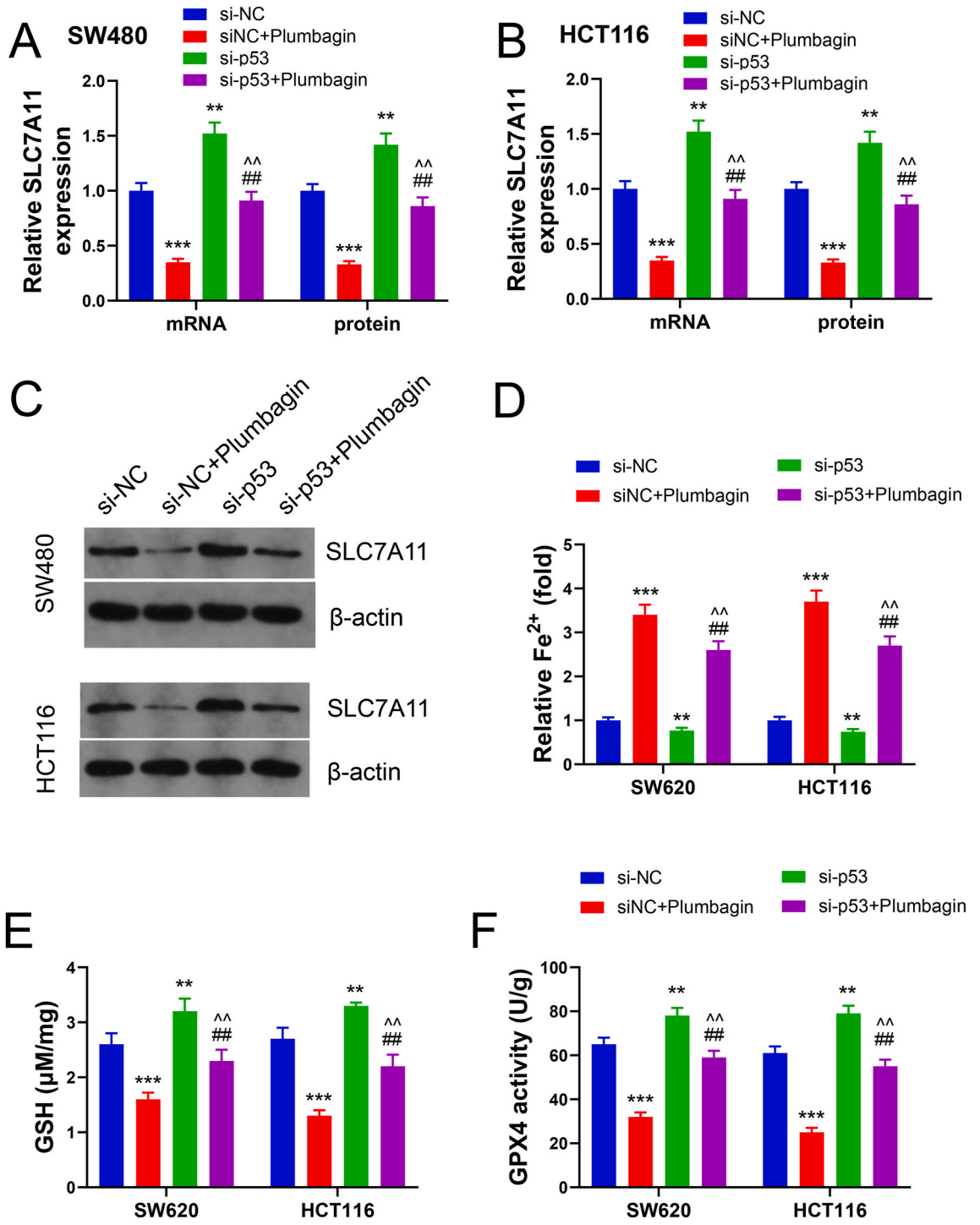

Fig. 6. Silencing p53 blocks Plumbagin-induced suppression of SLC7A11 expression and ferroptosis. (A–B) Effects of silencing p53 and/or Plumbagin on SLC7A11 mRNA and protein expression. (D) Effects of silencing p53 and/or Plumbagin on Fe^{2+} concentration in cells. (E–F) Effects of silencing p53 and/or Plumbagin on GSH and GPX4 levels. **, ***P < 0.01, 0.001 vs. si-NC; ##P < 0.01 vs. si-NC + Plumbagin; ^^P < 0.01 vs. si-p53.

increase in SLC7A11 expression subsequent to a decrease in p53 expression enhances the drug resistance of oesophageal cancer cells [53]. Tanshinone IIA-induced reduction in SLC7A11 expression has been associated with increased p53 expression in gastric cancer cells [54]. In addition, upregulated p53 causes ferroptosis and decreased the level of SLC7A11 in osteosarcoma and prostate cancers [55,56]. p53 mutation has not been reported in SW480 and HCT116 cells used in this study. Treatment with plumbagin promoted the

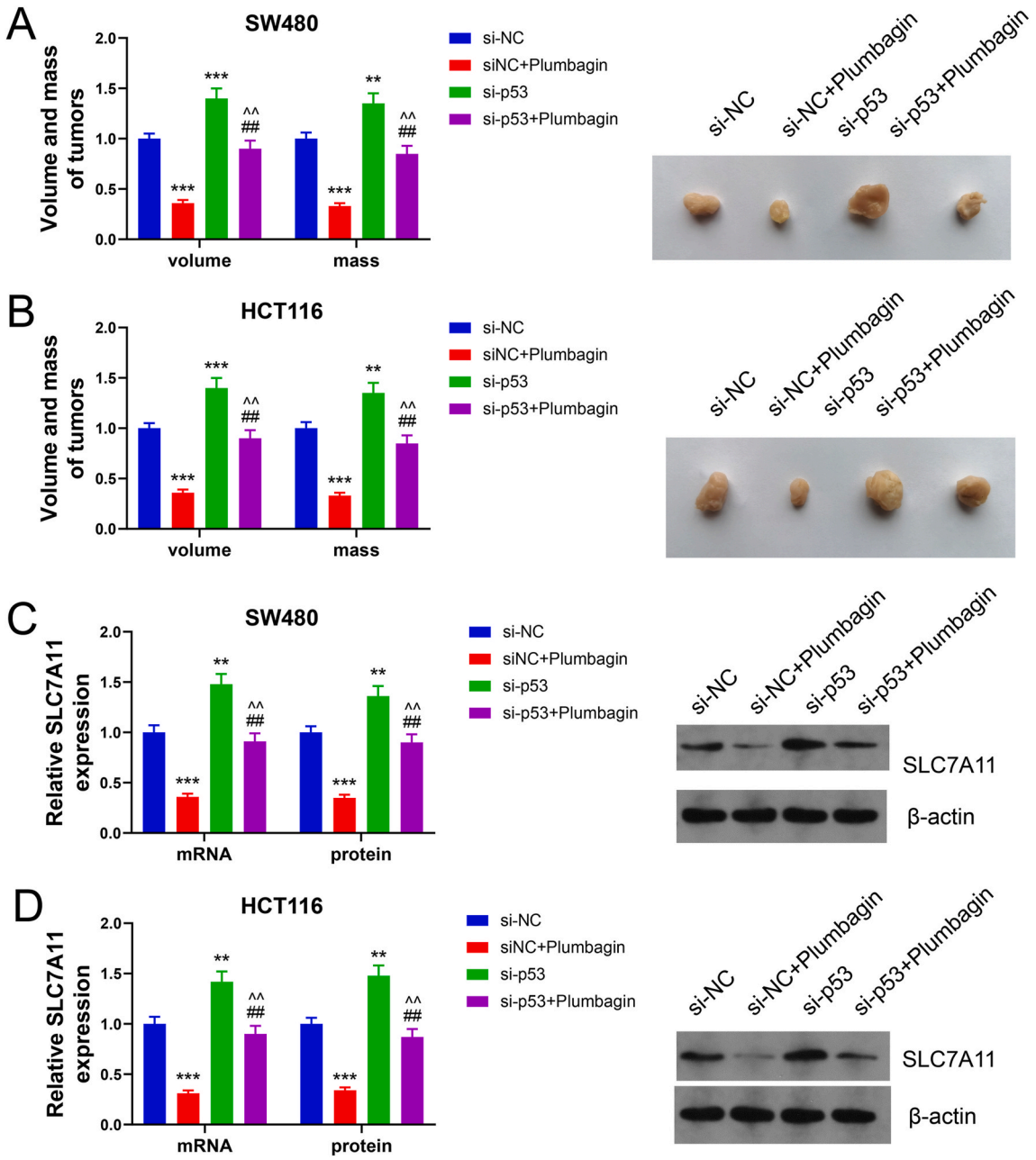

Fig. 7. Silencing of p53 blocks the in vivo anticancer effects of Plumbagin and inhibition of SLC7A11. (A–B) Effects of silencing p53 and/or Plumbagin on tumor volume and mass. (C–D) Effects of silencing p53 and/or Plumbagin on SLC7A11 mRNA and protein in tumor tissues. **, ***P < 0.01, 0.001 vs. si-NC; ##P < 0.01 vs. si-NC + Plumbagin; ^^P < 0.01 vs. si-p53.

expression of p-p53 and p53 and inhibited the expression of SLC7A11 in SW480 and HCT116 cells. However, silencing of p53 significantly blocked the ferroptosis-inducing effects of plumbagin and reversed its inhibitory effects on colon cancer cell. Plumbagin also exerted excellent anti-cancer effects and inhibited the protein expression of SLC7A11 in nude mice with colon cancer. Silencing of p53 attenuated the inhibitory effects of plumbagin on tumour growth and SLC7A11 expression and restored the levels of GSH and GPX4 in mice with colon cancer. In breast and lung cancers, the tumour-suppressing effects of plumbagin have been associated with its function of inducing p53 expression [57,58]. Notably, although plumbagin could inhibit the colony-forming and invasive abilities of colon cancer cells after p53 was silenced, its inhibitory effects were significantly weakened. Therefore, we speculate that the action of plumbagin is not solely dependent on p53. Consistently, previous researches have demonstrated that the effects of plumbagin may be dependent on other proteins, such as HIF-1α, caspase-9 and LC3B [59–61]. In this study, silencing of p53 blocked the ferroptosis-inducing and anti-cancer effects of plumbagin, suggesting that the mechanism of action of plumbagin is at least partially

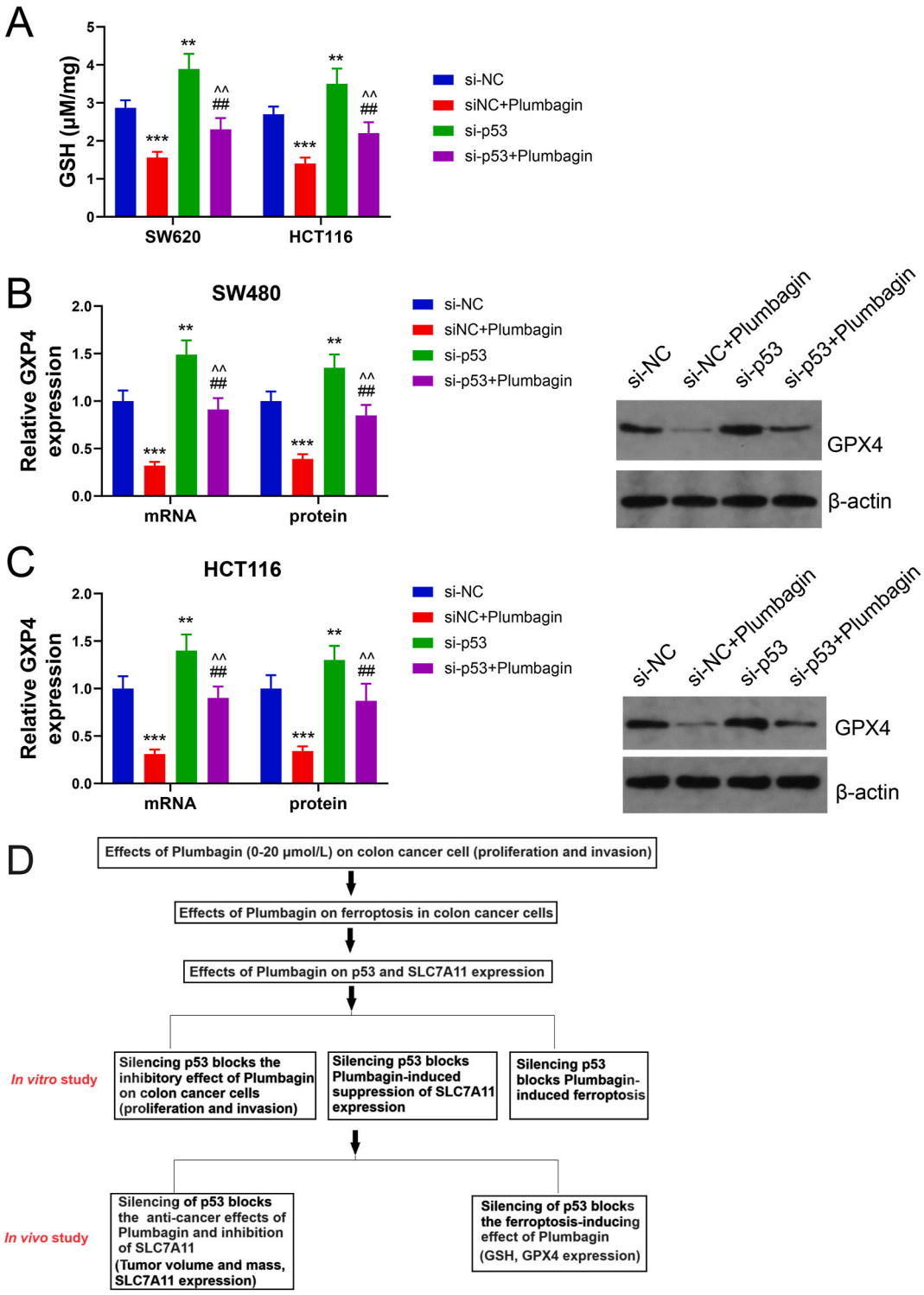

Fig. 8. Silencing of p53 blocks the ferroptosis-inducing effect of Plumbagin in vivo. (A) Effects of silencing p53 and/or Plumbagin on GSH levels in tumor tissues. (B–C) Effects of silencing p53 and/or Plumbagin on GPX4 mRNA and protein in tumor tissues. (D) A scheme that summarizes the main context of the paper. **, ***P < 0.01, 0.001 vs. si-NC; ##P < 0.01 vs. si-NC + Plumbagin; ^^P < 0.01 vs. si-p53.

related to p53–SLC7A11-dependent ferroptosis.

Certain limitations of this study should be recognized. First, plumbagin may induce ferroptosis through pathways other than p53; these pathways should be comprehensively investigated in future studies. For example, plumbagin has been reported to have tumour-suppressing effects on p53-mutated ovarian cancer [62]. Second, whether plumbagin exerts ferroptosis-inducing and anti-cancer effects on p53-mutated or -deleted colon cancer cells warrant further investigation, which is also the focus of our future research.

In conclusion, plumbagin can promote ferroptosis and inhibit cell proliferation and invasion in colon cancer (p53 wild-type). Mechanistically, plumbagin exerts anti-cancer effects by reducing the expression of SLC7A11 protein through the p53 pathway. Therefore, plumbagin may serve as a promising drug for certain genotypes of colon cancer.

Ethics statement

The animal study was approved by the ethical committee of Tongren Hospital (No. 2021TR0365).

Funding

Funding for the present study was provided by the Natural Science Foundation Project of the Medical College at Shanghai Jiaotong University.

Data availability statement

Data will be provided by the corresponding author upon request.

CRediT authorship contribution statement

Bingyi Wang: Writing – original draft, Methodology, Investigation, Data curation, Conceptualization. **Weiqi Kong:** Methodology, Investigation, Formal analysis, Data curation. **Lixin Lv:** Visualization, Validation, Software, Methodology. **Zhiqiang Wang:** Writing – review & editing, Validation, Supervision, Project administration, Funding acquisition, Data curation, Conceptualization.

Declaration of competing interest

There is no conflict of interest.

Appendix A. Supplementary data

Supplementary data to this article can be found online at https://doi.org/10.1016/j.heliyon.2024.e28364.

References

[1] H. Sung, et al., Global cancer statistics 2020: GLOBOCAN estimates of incidence and mortality worldwide for 36 cancers in 185 countries, CA Cancer J Clin 71 (3) (2021) 209–249.
[2] M. Chalabi, et al., Neoadjuvant immunotherapy leads to pathological responses in MMR-proficient and MMR-deficient early-stage colon cancers, Nat Med 26 (4) (2020) 566–576.
[3] A.E. Snook, et al., Split tolerance permits safe Ad5-GUCY2C-PADRE vaccine-induced T-cell responses in colon cancer patients, J Immunother Cancer 7 (1) (2019) 104.
[4] E.L. Van Blarigan, et al., Association of survival with adherence to the American cancer society nutrition and physical activity guidelines for cancer survivors after colon cancer diagnosis: the CALGB 89803/alliance trial, JAMA Oncol. 4 (6) (2018) 783–790.
[5] T. Yoshino, et al., Pan-Asian adapted ESMO Clinical Practice Guidelines for the diagnosis treatment and follow-up of patients with localised colon cancer, Ann. Oncol. 32 (12) (2021) 1496–1510.
[6] C. Kim, B. Kim, Anti-cancer natural products and their bioactive compounds inducing er stress-mediated apoptosis: a review, Nutrients 10 (8) (2018).
[7] D.J. Newman, G.M. Cragg, Natural products as sources of new drugs over the nearly four decades from 01/1981 to 09/2019, J Nat Prod 83 (3) (2020) 770–803.
[8] N. Sakunrangsit, W. Ketchart, Plumbagin inhibits cancer stem-like cells, angiogenesis and suppresses cell proliferation and invasion by targeting Wnt/β-catenin pathway in endocrine resistant breast cancer, Pharmacol. Res. 150 (2019) 104517.
[9] S.K. Tripathi, K.R.R. Rengasamy, B.K. Biswal, Plumbagin engenders apoptosis in lung cancer cells via caspase-9 activation and targeting mitochondrial-mediated ROS induction, Arch Pharm. Res. (Seoul) 43 (2) (2020) 242–256.
[10] J.Y. Tian, et al., PSMA conjugated combinatorial liposomal formulation encapsulating genistein and plumbagin to induce apoptosis in prostate cancer cells, Colloids Surf. B Biointerfaces 203 (2021) 111723.
[11] B. Eldhose, et al., Plumbagin reduces human colon cancer cell survival by inducing cell cycle arrest and mitochondria-mediated apoptosis, Int. J. Oncol. 45 (5) (2014) 1913–1920.
[12] Y. Sun, et al., The emerging role of ferroptosis in inflammation, Biomed. Pharmacother. 127 (2020) 110108.
[13] Z. Tang, et al., Deubiquitinase USP35 modulates ferroptosis in lung cancer via targeting ferroportin, Clin. Transl. Med. 11 (4) (2021) e390.
[14] C.A. Wohlhieter, et al., Concurrent mutations in STK11 and KEAP1 promote ferroptosis protection and SCD1 dependence in lung cancer, Cell Rep. 33 (9) (2020) 108444.
[15] X. Cheng, et al., SLC7A11, a potential therapeutic target through induced ferroptosis in colon adenocarcinoma, Front. Mol. Biosci. 9 (2022) 889688.
[16] X. Wang, et al., Stem cell factor SOX2 confers ferroptosis resistance in lung cancer via upregulation of SLC7A11, Cancer Res. 81 (20) (2021) 5217–5229.
[17] J. Yang, et al., Metformin induces Ferroptosis by inhibiting UFMylation of SLC7A11 in breast cancer, J. Exp. Clin. Cancer Res. 40 (1) (2021) 206.

[18] X. Zhang, J. Zhao, P. Xie, S. Wang, Biomedical applications of electrets: recent advance and future perspectives, J. Funct. Biomater. 14 (6) (2023) 320.
[19] D.N. Jackson, A.L. Theiss, Gut bacteria signaling to mitochondria in intestinal inflammation and cancer, Gut Microb. 11 (3) (2020) 285–304.
[20] E.E. Low, et al., Risk factors for early-onset colorectal cancer, Gastroenterology 159 (2) (2020) 492–501.e7.
[21] J. Tie, et al., Circulating tumor DNA analyses as markers of recurrence risk and benefit of adjuvant therapy for stage III colon cancer, JAMA Oncol. 5 (12) (2019) 1710–1717.
[22] J.A. Meyerhardt, et al., Effect of celecoxib vs placebo added to standard adjuvant therapy on disease-free survival among patients with stage III colon cancer: the CALGB/SWOG 80702 (alliance) randomized clinical trial, JAMA 325 (13) (2021) 1277–1286.
[23] H.J. Schmoll, et al., Effect of adjuvant capecitabine or fluorouracil, with or without oxaliplatin, on survival outcomes in stage III colon cancer and the effect of oxaliplatin on post-relapse survival: a pooled analysis of individual patient data from four randomised controlled trials, Lancet Oncol. 15 (13) (2014) 1481–1492.
[24] C. Kaltenmeier, et al., Time to surgery and colon cancer survival in the United States, Ann. Surg. 274 (6) (2021) 1025–1031.
[25] E. Rosander, et al., Preoperative multidisciplinary team assessment is associated with improved survival in patients with locally advanced colon cancer; a nationwide cohort study in 3157 patients, Eur. J. Surg. Oncol. 47 (9) (2021) 2398–2404.
[26] Y. Yuan, et al., Neoadjuvant chemoradiotherapy for patients with unresectable radically locally advanced colon cancer: a potential improvement to overall survival and decrease to multivisceral resection, BMC Cancer 21 (1) (2021) 179.
[27] D. Kashyap, et al., Natural product-based nanoformulations for cancer therapy: opportunities and challenges, Semin. Cancer Biol. 69 (2021) 5–23.
[28] S. Pothongsrisit Iksen, V. Pongrakhananon, Targeting the PI3K/AKT/mTOR signaling pathway in lung cancer: an update regarding potential drugs and natural products, Molecules 26 (13) (2021).
[29] F.A. Qais, et al., Plumbagin inhibits quorum sensing-regulated virulence and biofilms of Gram-negative bacteria: in vitro and in silico investigations, Biofouling 37 (7) (2021) 724–739.
[30] K. Zhang, et al., Plumbagin suppresses dendritic cell functions and alleviates experimental autoimmune encephalomyelitis, J. Neuroimmunol. 273 (1–2) (2014) 42–52.
[31] Y. Alharbi, et al., Oxidative stress induced by the anti-cancer agents, plumbagin, and atovaquone, inhibits ion transport through Na(+)/K(+)-ATPase, Sci. Rep. 10 (1) (2020) 19585.
[32] K. Pandey, et al., Prooxidative activity of plumbagin induces apoptosis in human pancreatic ductal adenocarcinoma cells via intrinsic apoptotic pathway, Toxicol. Vitro 65 (2020) 104788.
[33] R. Zhou, et al., Bioinformatic and experimental data decipher the pharmacological targets and mechanisms of plumbagin against hepatocellular carcinoma, Environ. Toxicol. Pharmacol. 70 (2019) 103200.
[34] Y.Y. Cao, et al., Plumbagin inhibits the proliferation and survival of esophageal cancer cells by blocking STAT3-PLK1-AKT signaling, Cell Death Dis. 9 (2) (2018) 17.
[35] C. Yang, et al., Plumbagin inhibits tumor angiogenesis of gastric carcinoma in mice by modulating nuclear factor-kappa B pathway, Transl. Cancer Res. 9 (2) (2020) 556–564.
[36] M.B. Chen, et al., Activation of AMP-activated protein kinase (AMPK) mediates plumbagin-induced apoptosis and growth inhibition in cultured human colon cancer cells, Cell. Signal. 25 (10) (2013) 1993–2002.
[37] M.Y. Hsu, et al., Iron: an essential element of cancer metabolism, Cells 9 (12) (2020).
[38] A. Diallo, et al., Dietary iron intake and breast cancer risk: modulation by an antioxidant supplementation, Oncotarget 7 (48) (2016) 79008–79016.
[39] K. Komoto, et al., Iron chelation cancer therapy using hydrophilic block copolymers conjugated with deferoxamine, Cancer Sci. 112 (1) (2021) 410–421.
[40] H. Yu, et al., Sulfasalazine-induced ferroptosis in breast cancer cells is reduced by the inhibitory effect of estrogen receptor on the transferrin receptor, Oncol. Rep. 42 (2) (2019) 826–838.
[41] C. Liang, et al., Recent progress in ferroptosis inducers for cancer therapy, Adv Mater 31 (51) (2019) e1904197.
[42] G.Q. Chen, et al., Artemisinin compounds sensitize cancer cells to ferroptosis by regulating iron homeostasis, Cell Death Differ. 27 (1) (2020) 242–254.
[43] C. Li, et al., Circ_0008035 contributes to cell proliferation and inhibits apoptosis and ferroptosis in gastric cancer via miR-599/EIF4A1 axis, Cancer Cell Int. 20 (1) (2020) 84.
[44] X. Tang, et al., Curcumin induces ferroptosis in non-small-cell lung cancer via activating autophagy, Thorac Cancer 12 (8) (2021) 1219–1230.
[45] S. Zhan, et al., Targeting NQO1/GPX4-mediated ferroptosis by plumbagin suppresses in vitro and in vivo glioma growth, Br. J. Cancer 127 (2) (2022) 364–376.
[46] M. Gao, J. Yi, J. Zhu, A.M. Minikes, P. Monian, C.B. Thompson, X. Jiang, Role of mitochondria in ferroptosis, Mol Cell. 73 (2) (2019 Jan 17) 354–363.e3. Tang D, Kroemer G. Ferroptosis. Curr Biol. 2020 Nov 2;30(21):R1292-R1297.
[47] S. Doll, B. Proneth, Y.Y. Tyurina, E. Panzilius, S. Kobayashi, I. Ingold, M. Irmler, J. Beckers, M. Aichler, A. Walch, H. Prokisch, D. Trümbach, G. Mao, F. Qu, H. Bayir, J. Füllekrug, C.H. Scheel, W. Wurst, J.A. Schick, V.E. Kagan, J.P. Angeli, M. Conrad, ACSL4 dictates ferroptosis sensitivity by shaping cellular lipid composition, Nat. Chem. Biol. 13 (1) (2017 Jan) 91–98.
[48] D. Tang, G. Kroemer, Ferroptosis, Curr. Biol. 30 (21) (2020 Nov 2) R1292–R1297.
[49] M.M. Gaschler, A.A. Andia, H. Liu, J.M. Csuka, B. Hurlocker, C.A. Vaiana, D.W. Heindel, D.S. Zuckerman, P.H. Bos, E. Reznik, L.F. Ye, Y.Y. Tyurina, A.J. Lin, M. S. Shchepinov, A.Y. Chan, E. Peguero-Pereira, M.A. Fomich, J.D. Daniels, A.V. Bekish, V.V. Shmanai, V.E. Kagan, L.K. Mahal, K.A. Woerpel, B.R. Stockwell, FINO2 initiates ferroptosis through GPX4 inactivation and iron oxidation, Nat. Chem. Biol. 14 (5) (2018 May) 507–515.
[50] H. Chen, et al., Patulin disrupts SLC7A11-cystine-cysteine-GSH antioxidant system and promotes renal cell ferroptosis both in vitro and in vivo, Food Chem. Toxicol. 166 (2022) 113255.
[51] M. Baradat, et al., 4-Hydroxy-2(E)-nonenal metabolism differs in Apc(+/+) cells and in Apc(Min/+) cells: it may explain colon cancer promotion by heme iron, Chem. Res. Toxicol. 24 (11) (2011) 1984–1993.
[52] S. Chen, et al., Endogenous hydrogen sulfide regulates xCT stability through persulfidation of OTUB1 at cysteine 91 in colon cancer cells, Neoplasia 23 (5) (2021) 461–472.
[53] A.K. Eichelmann, et al., Mutant p53 mediates sensitivity to cancer treatment agents in oesophageal adenocarcinoma associated with MicroRNA and SLC7A11 expression, Int. J. Mol. Sci. 22 (11) (2021).
[54] Z. Guan, et al., Tanshinone IIA induces ferroptosis in gastric cancer cells through p53-mediated SLC7A11 down-regulation, Biosci. Rep. 40 (8) (2020).
[55] Y. Luo, et al., Bavachin induces ferroptosis through the STAT3/P53/slc7a11 Axis in osteosarcoma cells, Oxid. Med. Cell. Longev. 2021 (2021) 1783485.
[56] X. Zhou, et al., Flubendazole, FDA-approved anthelmintic, elicits valid antitumor effects by targeting P53 and promoting ferroptosis in castration-resistant prostate cancer, Pharmacol. Res. 164 (2021) 105305.
[57] U. De, et al., Plumbagin from a tropical pitcher plant (Nepenthes alata Blanco) induces apoptotic cell death via a p53-dependent pathway in MCF-7 human breast cancer cells, Food Chem. Toxicol. 123 (2019) 492–500.
[58] Y.L. Hsu, et al., Plumbagin (5-hydroxy-2-methyl-1,4-naphthoquinone) induces apoptosis and cell cycle arrest in A549 cells through p53 accumulation via c-Jun NH2-terminal kinase-mediated phosphorylation at serine 15 in vitro and in vivo, J Pharmacol Exp Ther 318 (2) (2006) 484–494.
[59] S. Jampasri, S. Reabroi, D. Tungmunnithum, W. Parichatikanond, D. Pinthong, Plumbagin suppresses breast cancer progression by downregulating HIF-1α expression via a PI3K/Akt/mTOR independent pathway under hypoxic condition, Molecules 27 (17) (2022 Sep 5) 5716.
[60] S.K. Tripathi, K.R.R. Rengasamy, B.K. Biswal, Plumbagin engenders apoptosis in lung cancer cells via caspase-9 activation and targeting mitochondrial-mediated ROS induction, Arch Pharm. Res. (Seoul) 43 (2) (2020 Feb) 242–256.
[61] V.S. Periasamy, J. Athinarayanan, G. Ramankutty, M.A. Akbarsha, A.A. Alshatwi, Plumbagin triggers redox-mediated autophagy through the LC3B protein in human papillomavirus-positive cervical cancer cells, Arch. Med. Sci. 18 (1) (2020 Nov 20) 171–182.
[62] S. Sinha, et al., Plumbagin inhibits tumorigenesis and angiogenesis of ovarian cancer cells in vivo, Int. J. Cancer 132 (5) (2013) 1201–1212.